Passive polarization rotator based on silica photonic crystal fiber for 1.31-μm and 1.55-μm bands via adjusting the fiber length*

Chen Lei(陈 雷), Zhang Wei-Gang(张伟刚)†, Wang Li(王 丽), Bai Zhi-Yong(白志勇), Zhang Shan-Shan(张珊珊), Wang Biao(王 标), Yan Tie-Yi(严铁毅), and Jonathan Sieg

Key Laboratory of Optical Information Science and Technology, Ministry of Education, Institute of Modern Optics, Nankai University, Tianjin 300071, *China*

(Received 24 December 2013; revised manuscript received 7 March 2014; published online 10 August 2014)

A new polarization rotator based on the silica photonic crystal fiber is proposed. The proposed polarization rotator photonic crystal fiber (PR-PCF) possesses a triangle jigsaw-shape core region. The full-vector finite-element method is used to analyze the phenomenon of polarization conversion between the quasi-TE and quasi-TM modes. Numerical simulations show that the wavelengths of 1.31 μm and 1.55 μm are converted with a nearly 100% polarization conversion ratio with their matched coupling length and has a relatively strong realistic fabrication tolerance – 100 nm on the *y* axis and 50 nm on the *x* axis. The full vectorial finite difference beam propagation method is used to confirm the performance of the proposed PR-PCF.

Keywords: polarization rotation, photonic crystal fibers, beam propagation method, full-vector finite-element method

PACS: 42.81.Gs, 42.79.–e, 42.82.Bq, 42.81.–i **DOI:** 10.1088/1674-1056/23/10/104220

1. Introduction

The polarization rotator (PR) is very important for modern integrated optical circuits, such as in polarization modulators,[1] polarization switches,[2] and polarization splitters.[3–9] Over the years, many different kinds of PRs have been reported in the academic literature. For example, a multi-section structure with a periodically alternating asymmetric waveguide made of InP can realize PR in 1.3-μm bands with about 80% polarization conversion ratio;[10] a grating assisted codirectional coupler consisting of segments of asymmetrically etched ridge waveguides by using SiON technology realizes PR at 0.655-μm bands with over 98% polarization conversion ratio;[11] a multi-section structure with periodically alternating side wall waveguide made of InP and InGaAsP can operate over the 1.53 μm–1.61 μm wavelength range with a polarization conversion of more than 99%;[12] a photonic crystal fiber (PCF) filled with liquid crystal can achieve electrically tunable PR in an operating wavelength range of 1.55 μm, and a nearly 100% polarization conversion would be achieved;[13] and silica PCF with a rectangular core region combined with a slanted sidewall offers almost a 100% polarization conversion ratio.[14,15] Because the 1.31-μm and 1.55-μm wavelength bands are the most commonly used communication windows for the wavelength division multiplexer (WDM), which is a key component in modern integrated optical circuit systems, many studies have focused on the design and realization of a dual wavelength PCF to simultaneously operate on two communication windows — 1.31 μm and 1.55 μm serving as optical fiber communication and sensor, such as the measurement of temperature and force based on filling liquids with different indexes into a PCF[16] and single polarization wavelength splitters.[3–5]

However, all reported PRs whose operating wavelengths can serve at most one of the two communication wavelengths need further development. Meanwhile, these structures each have a relatively weak realistic fabrication tolerance. To further develop PR, in this paper we first propose and design a PR-PCF with a triangle jigsaw (TJ) shape core region. This design can operate over a large wavelength span covering two communication windows for 1.31-μm and 1.55-μm bands with their matched length, and this unique characteristic will have great applications in high sensitivity sensors, high-power fiber lasers, mode-locked lasers, and future optical fiber communication systems. In addition, we propose, according to the theoretical analysis and numerical simulation, that the designed PR-PCF has a high polarization conversion ratio section at each communication window that gives a relatively strong realistic fabrication tolerance to that design — 100 nm on the *y* axis and 50 nm on the *x* axis.

2. Fiber design and analysis

This novel PR-PCF with a TJ shape core region is realized by means of a constructive interference between the two polarization modes (fundamental mode). When a light beam with

*Project supported by the National Natural Science Foundation of China (Grant Nos. 11274181, 10974100, 61203204, and 10674075), the Doctoral Scientific Fund Project of the Ministry of Education of China (Grant No. 20120031110033), and the Tianjin Key Program of Application Foundations and Future Technology Research Project, China (Grant No. 10JCZDJC24300).

†Corresponding author. E-mail: zhangwg@nankai.edu.cn

© 2014 Chinese Physical Society and IOP Publishing Ltd

transverse electric/transverse magnetic mode (TE/TM mode) inputs the PR-PCF, the fundamental quasi-TE and quasi-TM modes possessing different propagation constants are stimulated, which are coupled with each other after propagating a coupling length.[4,14,15] For clarity, the fundamental quasi-TE and fundamental quasi-TM modes are called quasi-TE mode and quasi-TM mode respectively. The phase mismatch between the two modes for two orthogonal polarization states will vary with the propagation distance. When the phase-mismatch is reached, whose corresponding propagation distance is defined as the coupling wavelength (L_π), nearly pure TM/TE modes can be collected from the PR-PCF output. The coupling length for the two modes is given by[4,17]

$$L_\pi = \frac{\pi}{\beta_{\mathrm{TE}} - \beta_{\mathrm{TM}}} = \frac{\lambda}{2(n_{\mathrm{TE}} - n_{\mathrm{TM}})}, \tag{1}$$

where β_{TE} and β_{TM} are the propagation constants of the quasi-TE and quasi-TM modes, n_{TE} and n_{TM} are the effective indexes of the quasi-TE and quasi-TM modes respectively. If the modal hybrid components of the two modes are identical, the energies of the quasi-TE and quasi-TM modes are equally distributed, which means the polarization rotator can be made.

In this study, the modal hybrid component is defined based on physical reality as follows:[18]

$$S = \iint [|E_x(\mathrm{TE},1)E_x(\mathrm{TE},2)| + |E_y(TE,1)E_y(TM,2)|]\,\mathrm{d}x\mathrm{d}y, \tag{2}$$

where E(TE, 1) and E(TM, 2) are the vector fields, respectively, for quasi-TE and quasi-TM modes in the input section of the proposed PR-PCF.

Figure 1(a) shows the cross-section diagram of the proposed PR-PCF with a TJ shape core region. Here, Λ_x and Λ_y are hole pitches on the x and y axes, and d refers to the diameter of the cladding air holes. The background refractive index is calculated from the Sellmeier equation.[12,19] We use the full-vector finite-element method (FEM) to analyze the phenomenon of polarization conversion between the quasi-TE and quasi-TM modes.[3–5]

Figures 1(b)–1(e) show the dominant and non-dominant electric field components of the quasi-TE and quasi-TM modes of the proposed PR-PCF with $\Lambda_x = 1.45$ μm, $\Lambda_y = 2.1$ μm, and $d = 1.4$ μm. It can be observed that the dominant and non-dominant component field profiles of the two modes at the operating wavelength 1.55 μm are very similar. This ensures that the proposed PR-PCF core region supports highly hybrid modes, which can be used for designing polarization conversion devices.

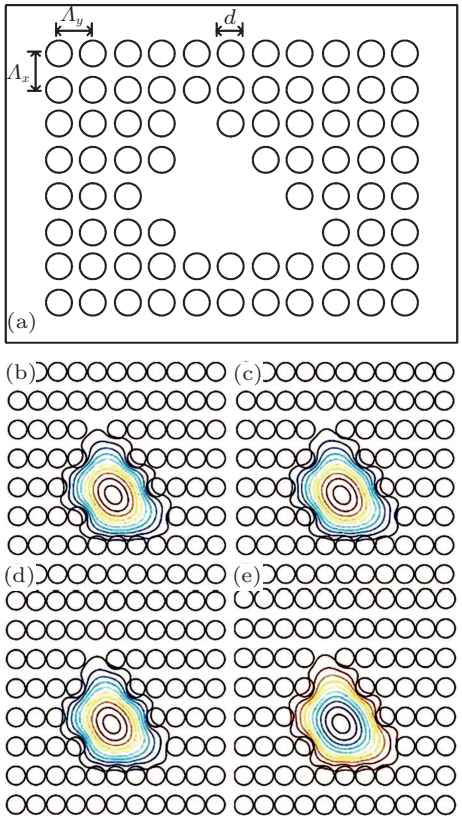


Fig. 1. (color online) (a) Cross-section diagram of the proposed PR-PCF; (b) contour plot of non-dominant E_x and (c) dominant E_y field profile of the fundamental quasi-TE mode; (d) contour plot of the non-dominant E_x and (e) dominant E_y field profile of the fundamental quasi-TM mode.

Since the modal hybrid component of the suggested PR can be affected by the hole pitches on the x and y axes, Λ_x and Λ_y vary from 1.45 μm to 2.8 μm and 1.45 μm to 1.75 μm while incrementally increasing by 0.05 μm in order to investigate the modal hybrid component. In the simulations, the diameter of the air hole in the cladding is taken to be 1.4 μm. Figures 2(a)—2(c) show the variations of the modal hybrid components and the conversion lengths with hole pitches at 1.31 μm and 1.55 μm. It can be seen from Fig. 2(a) that when Λ_x is fixed, the modal hybrid components of the two bands increase to a maximum value with Λ_y increasing, and then decrease as Λ_y further increases. The same trend can be easily found when Λ_y is fixed, and the two curves possess similar maximum values. Figure 2(b) shows the contour of Fig. 2(a). From Fig. 2(b), we can see that each wavelength has a section where the modal hybrid components are over 0.995. We choose two overlap sections possessed by two wavelengths. That combination can maintain the PR-PCF polarization conversion ratio over 0.995 in both bands. Moreover, it is evident from Fig. 2(b) that if we select the center of the overlap section as the optimized curve, even the fluctuations of Λ_x and Λ_y values increase up to about 50 nm and 100 nm respectively, neither of them is consequential. And this characteristic means that this design has a strong realistic fabrication tolerance. Figure 2(c) shows the variation of the proposed PR-PCF

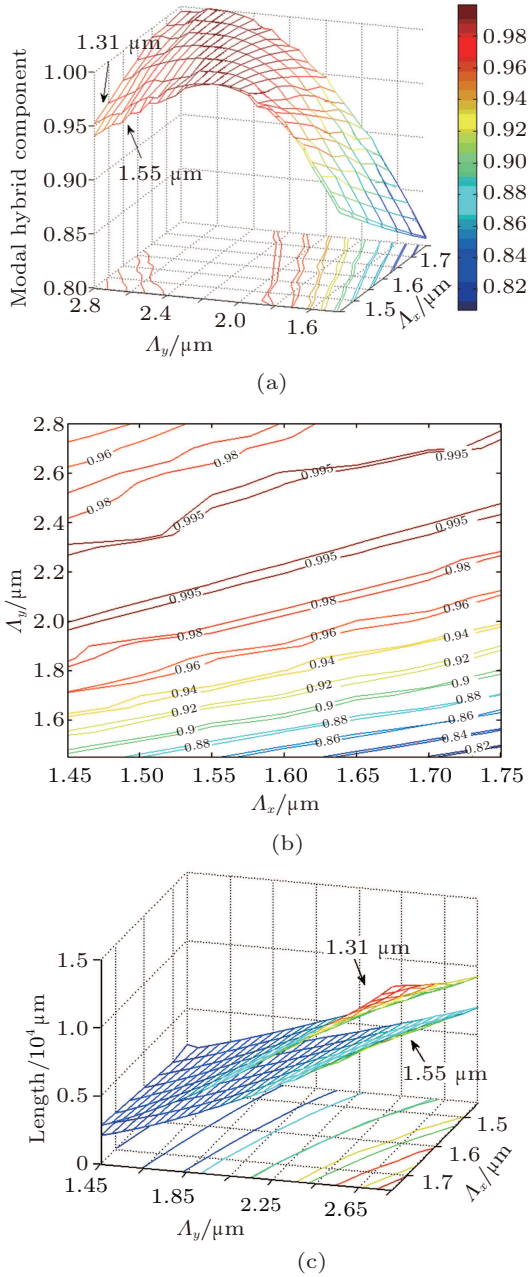


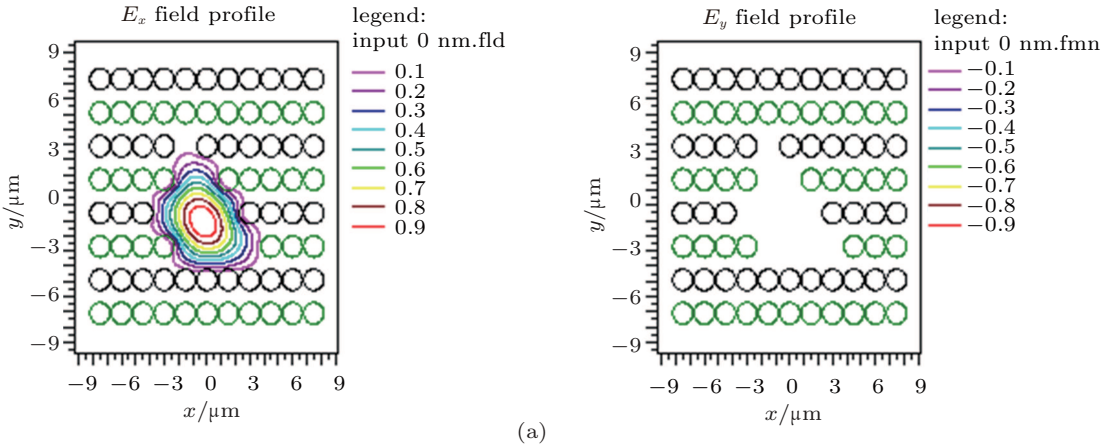
Fig. 2. (color online) Variations of (a) the hybrid components and (b) their projections with the hole pitch on the x and y axes; (c) variations of the conversion lengths with the hole pitch on the x and y axes.

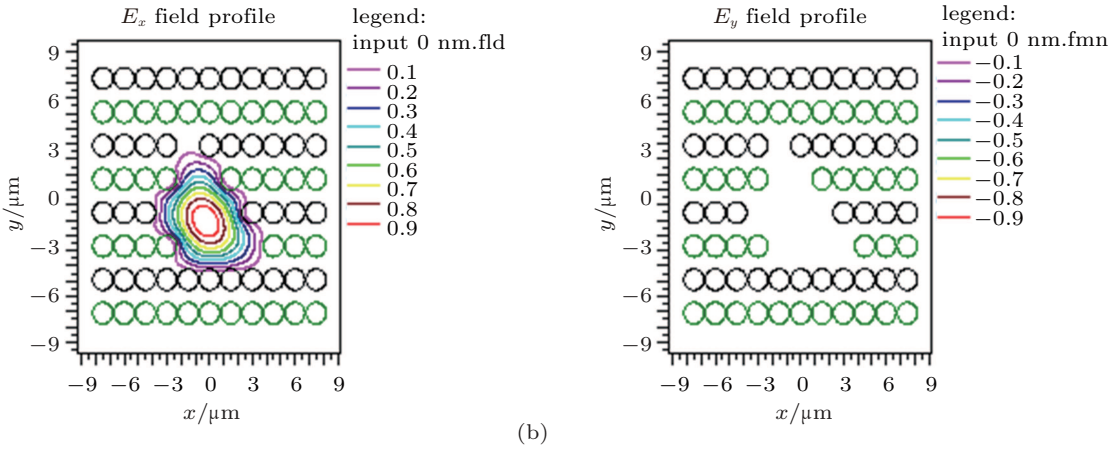
length with Λ_x and Λ_y values in the two bands. It can be seen that the length of the proposed PR-PCF must be increased to match the values of Λ_x and Λ_y.

To visualize the performance of the proposed PR-PCF, we plot the electric field distribution by using the full vectorial finite difference beam propagation method (FVFD-BPM).[20] We only select $\Lambda_x = 1.5$ μm and $\Lambda_y = 2.2$ μm as an example to confirm the performance of the proposed PR-PCF. Figures 3(a)–3(e) show contour patterns for the E_x and E_y field profiles at different values of propagation length $z = 0$, $L_\pi/2$ (3060.5 μm at 1.31 μm and 2293 μm at 1.55 μm), and L_π (6121 μm at 1.31 μm and 4586 μm at 1.55 μm). The calculated values of coupled length L_π by using the FEM are 6121 μm at the operating wavelength of 1.31 μm and 4586 μm at the operating wavelength of 1.55 μm, which are in excellent agreement with the 6121 μm and 4586 μm calculated by the FVFD-BPM.

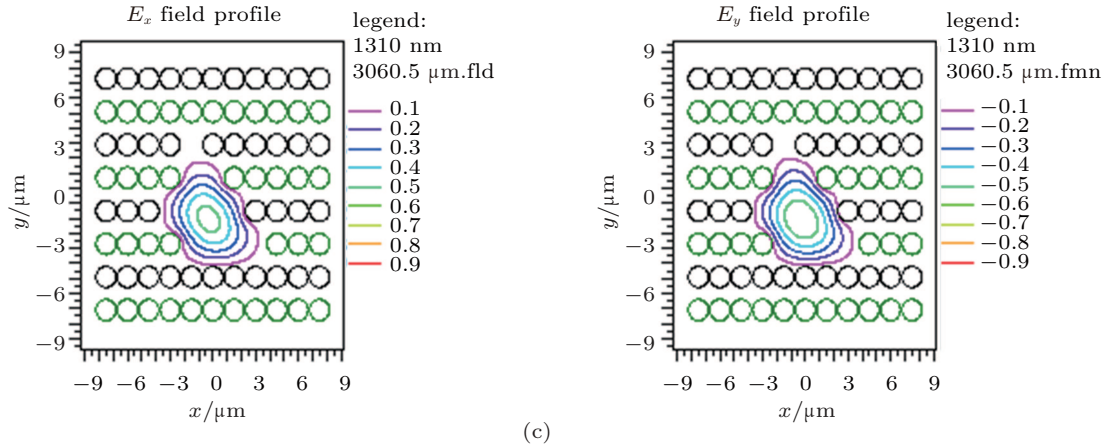
It can be observed from Fig. 3 that for TE mode of the simulations for the case of two wavelengths, initially the values for E_y are zero and then increase to maximum values at their matched coupled lengths. On the contrary, the values of E_x for the two wavelengths are initially at their corresponding maximum values and then decrease to their corresponding minimum values at their matched coupled lengths. As a consequence, input TE mode becomes output TM mode. Similarly, if TM mode inputs the PR-PCF, nearly pure TE mode can be collected from the PR-PCF output.

The crosstalk (CT) is a key parameter for PR rotators, which will determine the influence of unwanted polarization modes and thus can characterize the transmission performances. According to Ref. [4], the CT with the parameters of the above example can be calculated and the results are shown in Fig. 4. The dotted line with circles denote the CT when the fiber length is equal to the coupled length $L_\pi = 6121$ μm for 1.31 μm, the dashed line with squares represent the CT when the fiber length is equal to the coupled length $L_\pi = 4586$ μm

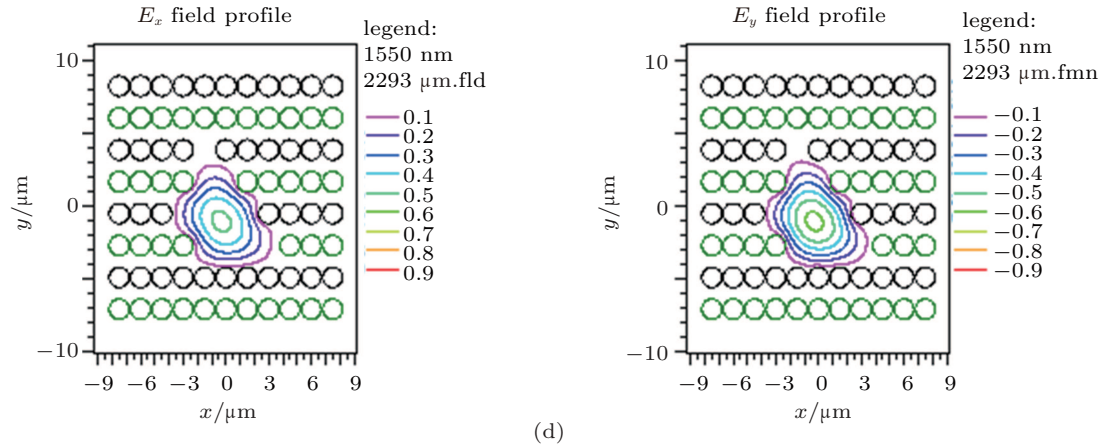



E_x field profile
legend:
input 0 nm.fld
0.1
0.2
0.3
0.4
0.5
0.6
0.7
0.8
0.9
$y/\mu m$
$x/\mu m$
E_y field profile
legend:
input 0 nm.fmn
−0.1
−0.2
−0.3
−0.4
−0.5
−0.6
−0.7
−0.8
−0.9

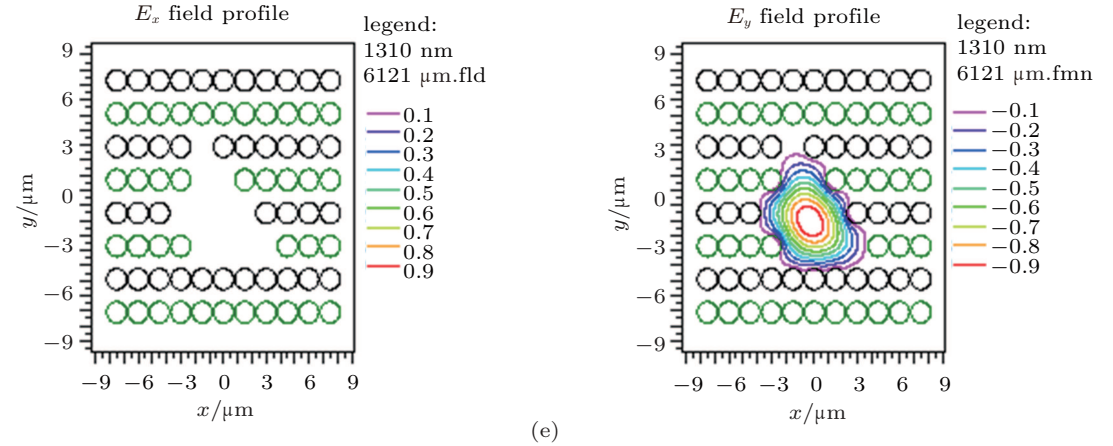
(b)


E_x field profile
legend:
1310 nm
3060.5 μm.fld
0.1
0.2
0.3
0.4
0.5
0.6
0.7
0.8
0.9
$y/\mu m$
$x/\mu m$
E_y field profile
legend:
1310 nm
3060.5 μm.fmn
−0.1
−0.2
−0.3
−0.4
−0.5
−0.6
−0.7
−0.8
−0.9

(c)


E_x field profile
legend:
1550 nm
2293 μm.fld
0.1
0.2
0.3
0.4
0.5
0.6
0.7
0.8
0.9
$y/\mu m$
$x/\mu m$
E_y field profile
legend:
1550 nm
2293 μm.fmn
−0.1
−0.2
−0.3
−0.4
−0.5
−0.6
−0.7
−0.8
−0.9

(d)


E_x field profile
legend:
1310 nm
6121 μm.fld
0.1
0.2
0.3
0.4
0.5
0.6
0.7
0.8
0.9
$y/\mu m$
$x/\mu m$
E_y field profile
legend:
1310 nm
6121 μm.fmn
−0.1
−0.2
−0.3
−0.4
−0.5
−0.6
−0.7
−0.8
−0.9

(e)

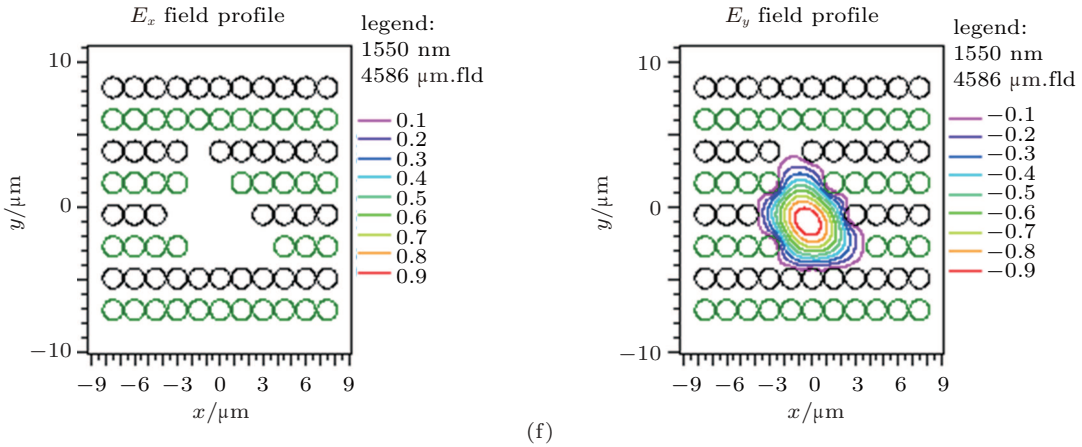


Fig. 3. (color online) Contour plots at 1.31 μm of E_x and E_y field profiles at propagation length $z = 0$ (a) and 3060.5 μm corresponding to $L_\pi/2$ for 1.31 μm (c); contour plots at 1.55 μm of E_x and E_y field profiles at propagation length $z = 0$ (b) and 2293 μm corresponding to $L_\pi/2$ for 1.55 μm (d); contour plot at 1.31 μm of E_x and E_y field profiles at propagation length $z = 6121$ μm corresponding to L_π for 1.31 μm (e); contour plot at 1.55 μm of E_x and E_y field profiles at propagation length $z = 4586$ μm corresponding to L_π for 1.55 μm (f).

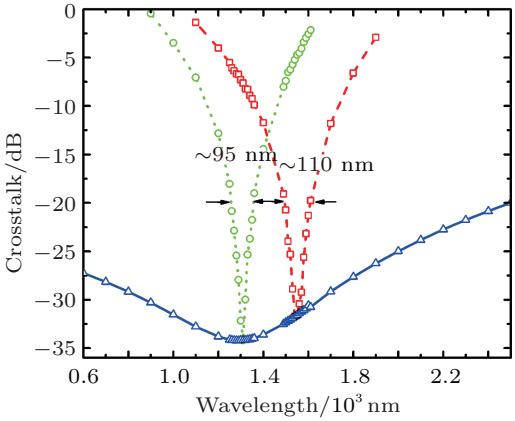


Fig. 4. (color online) Variation of crosstalk with wavelength for TE mode stimulation.

for 1.55 μm, and the solid line with triangles refer to the CT when the fiber length is equal to their matched coupled length L_π for all wavelengths ranging from 600 nm to 2500 nm respectively.

Here we consider the available optical bandwidth (BW) dependent on wavelength in a range within which the CT is lower than −20 dB. We can see that the proposed design can realize polarization conversion in a range from 600 nm to 2500 nm by adjusting the length of PR-PCF to their exact coupling length and has a reasonable BW [BW = 95 nm around 1.55 μm and BW = 105 nm around 1.31 μm] for their wavelength matched length.

3. Conclusion

In this paper, a passive polarization rotator based on silica PCF with a TJ shape core region is presented and analyzed. The numerical results demonstrate that the proposed design has the potential to provide almost 100% polarization conversion ratio in both 1.31-μm and 1.55-μm bands only by adjusting the length of the fiber. In addition, theoretical analysis and numerical simulation reveal that the proposed PR-PCF has a wavelength section with high polarization conversion ratio for each wavelength. And this advantage suggests that the designed PR-PCF possesses relatively strong realistic fabrication tolerances of about 100 nm and 50 nm on the y and x axes respectively. And, furthermore, we take a set of hole pitch parameters for example to analyze the crosstalk and confirm the performance of the proposed PR-PCF by using the FVFD-BPM.

References

[1] Heismann F and Smith R W 1994 *IEEE J. Sel. Top. Quantum Electron.* **2** 311
[2] Morita I, Tanaka K, Edagawa N and Suzuki M 1999 *IEEE J. Lightwave Technol.* **17** 2506
[3] Geng P C, Zhang W G, Gao S C, Zhang S S, Zhang H and Ruan J 2012 *IEEE Photon. Technol. Lett.* **24** 1304
[4] Zhang S S, Zhang W G, Geng P C, Li X L and Ruan J 2011 *Appl. Opt.* **50** 6576
[5] Geng P C, Zhang W G, Zhang H, Zhang S S, Ruan J, Wei S L and Xue X L 2012 *IEEE Photon. Technol. Lett.* **24** 452
[6] Sacher W D, Barwicz T, Taylor B J F and Poon J K S 2014 *Opt. Express* **22** 3777
[7] Wang J, Niu B, Sheng Z, Wu A M, Wang X, Zou S C, Qi M H and Gan F W 2014 *Opt. Express* **22** 4137
[8] Caspers J N, Alam M Z and Mojahedi M 2012 *Opt. Lett.* **37** 4615
[9] Ren G, Zheng W H, Wang K, Du X Y, Xing M X and Chen L H 2008 *Chin. Phys. B* **17** 1674
[10] Shani Y, Alferness R, Koch T, Koren U, Oron M, Miller B I and Young M G 1991 *Appl. Phys. Lett.* **59** 1278
[11] Koster T and Lambeck P 2001 *IEEE J. Lightwave Technol.* **19** 876
[12] Somasiri N, Rahman B M A and Obayya S S A 2002 *IEEE J. Lightwave Technol.* **20** 751
[13] Hameed M F O and Obayya S S A 2011 *IEEE J. Lightwave Technol.* **29** 2725
[14] Hameed M F O and Obayya S S A 2011 *Opt. Lett.* **36** 3133
[15] Hameed M F O, Obayya S S A and El-Mikati H A 2012 *IEEE J. Lightwave Technol.* **30** 283
[16] Liang H, Zhang W G, Geng P C, Liu Y G, Wang Z, Guo J Q, Gao S C and Yan S Y 2013 *Opt. Lett.* **38** 1071
[17] Liu X Y, Zhang F D, Zhang M and Ye P D 2005 *Chin. Phys.* **16** 1710
[18] Weinert C M and Heidrich H 1993 *IEEE Photon. Technol. Lett.* **5** 324
[19] Hameed M F O and Obayya S S A 2010 *IEEE J. Lightwave Technol.* **28** 806
[20] Huang W P and Xu C L 1993 *IEEE J. Quantum Electron.* **29** 2639